RT NO. 4 - GALCIT 101
ontract No. RU-293
July 1, 1959 - September 30, 1959

FUNDAMENTAL STUDIES RELATING TO SYSTEMS ANALYSIS OF SOLID PROPELLANTS

15 October 1959

Guggenheim Aeronautical Laboratory
California Institute of Technology
Pasadena, California

PROGRESS REPORT NO. 4 - GALCIT 101

Subcontract No. RU-293

July 1, 1959 - September 30, 1959

Fundamental Studies Relating to Systems Analysis of Solid Propellants

15 October 1959

P. J. Blatz
R. A. Schapery
L. D. Stimpson
M. L. Williams

This research is supported by
The Thiokol Chemical Corp., Redstone Division

Guggenheim Aeronautical Laboratory

California Institute of Technology

Pasadena, California

PREFACE

As in the previous progress reports, the contents in this report have been categorized so as to present a clear picture of their role in contributing to the problem of mechanical failure analysis. The subject of material representation by mechanical models is discussed in Section I, while Section II contains additions to the subject of Elastic Solutions for Cylinders. The Engineering Analysis section includes an example of the strain response of an internal star grain to pressure. A damped sinusoid has been assumed for the pressure rise, and the use of stress concentration factors for a star grain is demonstrated. Section V on failure includes some preliminary test results which indicate the feasibility of the cumulative damage concept for composite (polyurethene) propellants, at least in the limited range tested. Recommendations are given which would expand this testing to show how damage accumulates under other conditions such as low temperatures, high strain-rates and with other types of propellant.

Notation used throughout this report is defined within each section where used or consistent with that used in the previous reports, and hence defined there.

TABLE OF CONTENTS

I. MATERIAL BEHAVIOR

B. Fitting Model Parameters to Data

At the present time work is under way to determine a convenient method of obtaining approximate finite element models to represent propellant response. This includes both an investigation of experimental procedures as well as analytical techniques for fitting model parameters. While the program is not yet far enough along to present results in this report, one method suggested by Lee[4] will be discussed briefly. It should apply to both pressure and temperature loading problems if properties are assumed to be independent of time.

One first decomposes time dependence of the loading function (pressure or temperature) into harmonic components, and then determines the frequency range needed to represent the load adequately by a Fourier series. Strictly speaking, if the load is transient rather than periodic, one must use a Fourier integral. However, by spacing the periodic pulses far enough apart the response will be essentially the same as obtained with a single pulse.

After the appropriate frequency range is found, one next makes use of experimental data that gives the frequency dependence of pertinent moduli (or compliances) within this range. This data can sometimes be obtained in a direct way by applying a sinusoidally varying stress to a sample and recording the strain as a function of frequency. The ratio of stress to strain so obtained is called the complex modulus while its inverse is the complex compliance.* A suitable model is chosen and the complex modulus (or compliance) of the model is fitted to the experimental results over the frequency band determined in the first step. The complex modulus of a

---

*Due to the existence of viscosity, a sinusoidal stress $\sigma_0 e^{i\omega t}$ will not be in phase with the strain $\epsilon_0 e^{i\omega t}$, so that the ratio between stress and strain is given generally by a complex function of frequency (ω). If the complex modulus is denoted by $m^*(\omega)$, then

$$m^*(\omega) = \frac{\sigma}{\epsilon} = \frac{\sigma_0}{\epsilon_0} = m_1(\omega) + i\, m_2(\omega)$$

where $m_1(\omega)$ and $m_2(\omega)$ are the real and imaginary part of m^* respectively. Similarly, the complex compliance $k^*(\omega)$ is given by

$$k^*(\omega) = k_1(\omega) - i k_2(\omega) = \frac{1}{m^*(\omega)}$$

model is derived from the appropriate operator equation given in Table I of the second progress report[2] by replacing the time derivatives p by $i\omega$ where ω is the angular frequency and $i = \sqrt{-1}$. This last step prescribes the coefficients to be used in the operational modulus of the model.

In conclusion it may be emphasized that the above method does not necessarily require tests for direct determination of complex moduli. By using analytical relations, it should be possible to derive the complex quantities from other types of tests such as stress relaxation. The applicability of this latter technique is being studied.

II. ELASTIC SOLUTIONS FOR CYLINDERS

A-1. Extension of Elastic Solutions for Pressure to Cylinders with Internal Star-Shaped Perforations

Inasmuch as the stress and displacement solutions presented in the previous progress reports apply only to circularly perforated cylinders, it is useful to extend these solutions to include the more common star configurations (Figure II-1). An approximate method based upon elastic concentration factors will be discussed for both elastic and viscoelastic grains. In a paper by Ordahl and Williams[5] this method is applied to elastic grains (with and without cases) and several design curves are presented that give preliminary values of stress concentration factors.*

The concentration factor K has been defined[5] as

$$K = \frac{\sigma_r^s - \sigma_\theta^s}{\sigma_r - \sigma_\theta} \qquad \text{(II-1)}$$

where

σ_r^s, σ_θ^s = radial and tangential (hoop) principal stresses, respectively, in a star perforated grain.

σ_r, σ_θ = radial and tangential principal stresses, respectively, in a grain with a circular port.

The stresses σ_r and σ_θ, for either plane stress or the condition of constant strain ϵ_z, are given by[6]

$$\sigma_r = \left(\frac{b}{r}\right)^2 \frac{p' - p_i}{\left(\frac{b}{a}\right)^2 - 1} + \frac{p_i - \left(\frac{b}{a}\right)^2 p'}{\left(\frac{b}{a}\right)^2 - 1} \qquad \text{(II-2a)}$$

$$\sigma_\theta = -\left(\frac{b}{r}\right)^2 \frac{p' - p_i}{\left(\frac{b}{a}\right)^2 - 1} + \frac{p_i - \left(\frac{b}{a}\right)^2 p'}{\left(\frac{b}{a}\right)^2 - 1} \qquad \text{(II-2b)}$$

---

* The data was preliminary in the sense that only a limited amount of experimental values was used and that subsequent checks indicate about 20 °/o unconservative results. It is understood that other workers are presently engaged in refining the earlier data.

also

$$\sigma_r - \sigma_\theta = 2\left(\frac{b}{r}\right)^2 \frac{p' - p_i}{\left(\frac{b}{a}\right)^2 - 1} \qquad \text{(II-2c)}$$

where

p_i = internal pressure

p' = external pressure (for a case-bonded grain this is the pressure between the case and grain)

a = inside radius of circular grain

b = outside radius of circular grain

It is seen that ($\sigma_r - \sigma_\theta$) depends only on the pressure difference ($p' - p_i$); so that in order for K to be independent of loading ($\sigma_r^s - \sigma_\theta^s$) must also be proportional to ($p' - p_i$). This can be shown quite readily. Since linear behavior is assumed, σ_r^s and σ_θ^s are written generally as

$$\sigma_r^s = \beta_1 p_i + \beta_2 p' \qquad \text{(II-3a)}$$

$$\sigma_\theta^s = \beta_3 p_i + \beta_4 p' \qquad \text{(II-3b)}$$

in which β_1, β_2, β_3, and β_4 are geometrical factors pertaining to a particular configuration and, in general, are space dependent. It should be noted that these factors are independent of material properties since the stresses in (II-3) apply to a two dimensional problem with all stress boundary conditions. The stress difference is

$$\sigma_r^s - \sigma_\theta^s = (\beta_1 - \beta_3) p_i + (\beta_2 - \beta_4) p' \qquad \text{(II-4)}$$

A relationship between the β_i, which must hold for all pressures, can be found by considering the limit case of $p_i = p' = p$. When $p_i = p' = p$, a cylinder of any arbitrary cross-section is in a state of uniform hydrostatic pressure so that

$$\sigma_r^s = \sigma_\theta^s = -p$$

and therefore from (II-4) the β_i must satisfy

$$0 = (\beta_1 - \beta_3) + (\beta_2 - \beta_4)$$

or

$$(\beta_1 - \beta_3) = -(\beta_2 - \beta_4) \qquad \text{(II-5)}$$

Substitution of (II-5) into (II-4) yields

$$\sigma_r^s - \sigma_\theta^s = (\beta_2 - \beta_4)(p' - p_i) \tag{II-6}$$

which was to be shown.

The maximum stresses and strains occur at the star points, indicated in Figure II-1 and for this reason the necessary relations will be presented for calculating stresses and strains at this location only. It is clear that because of symmetry there is no shear stress acting along radial lines drawn thru the star points which means the stresses at the star points, denoted as σ_r^{sp} and σ_θ^{sp}, are principal stresses.

At the star point ($r = a$),

$K \equiv K_i$ (this corresponds to the notation of Ref. 5)

and

$$\sigma_r^{sp} = -p_i \tag{II-7}$$

Using (II-7), σ_θ^{sp} is found using (II-1) and (II-2c) evaluated at $r = a$:

$$\sigma_\theta^{sp} = K_i \left[\frac{2\left(\frac{b}{a}\right)^2}{\left(\frac{b}{a}\right)^2 - 1} \right] (p_i - p') - p_i \tag{II-8}$$

It is apparent from (II-8) that only when $p_i = 0$ can K_i be interpreted as the ratio of σ_θ^{sp} to σ_θ. It should be emphasized that the above results are independent of material properties if p_i and p' are known; thus, both viscoelastic and elastic stresses can be found using (II-7) and (II-8) with the values of K_i given in Ref. 5. However, with a case-bonded grain p' (assumed uniform) is the pressure between case and grain so that it is related to p_i thru geometrical factors and material properties. This necessitates the use of an approximation in which shear stresses at $r = b$ are neglected, and p' is assumed to be the same for both the star and circular configurations if the radius (a) of the circular port is made equal to the radius drawn to the star point. It is evident that this approximation improves as the web fraction $\frac{b-a}{b}$ increases.

Elastic solutions for p' are given in the first two progress reports[1, 2] for several pressure problems. With a viscoelastic grain it is necessary to solve a differential equation that arises when elastic constants in the equation for p' are replaced by appropriate differential operators. It may be noted that in general p_i and p' have the same time dependence only if the grain is elastic.

The radial, tangential, and axial strains at the star points, denoted as ϵ_r^{sp}, ϵ_θ^{sp}, and ϵ_z^{sp} respectively, are found by substituting (II-7) and (II-8) into the stress-strain equations:

$$\epsilon_r^{sp} = \frac{1}{E}\left[-P_i - \nu\left(\sigma_\theta^{sp} + \sigma_z^{sp}\right)\right] \tag{II-9a}$$

$$\epsilon_\theta^{sp} = \frac{1}{E}\left[\sigma_\theta^{sp} - \nu\left(-P_i + \sigma_z^{sp}\right)\right] \tag{II-9b}$$

$$\epsilon_z^{sp} = \frac{1}{E}\left[\sigma_z^{sp} - \nu\left(-P_i + \sigma_\theta^{sp}\right)\right] \tag{II-9c}$$

Two important cases can be distinguished: First, for plane stress ($\sigma_z = 0$)

$$\epsilon_r^{sp} = -\frac{1}{E}\left[(1-\nu)P_i + \nu K_i\left\{\frac{2\left(\frac{b}{a}\right)^2}{\left(\frac{b}{a}\right)^2 - 1}\right\}(P_i - P')\right] \tag{II-10a}$$

$$\epsilon_\theta^{sp} = \frac{1}{E}\left[-(1-\nu)P_i + K_i\left\{\frac{2\left(\frac{b}{a}\right)^2}{\left(\frac{b}{a}\right)^2 - 1}\right\}(P_i - P')\right] \tag{II-10b}$$

$$\epsilon_z^{sp} = -\frac{\nu}{E}\left[-2P_i + K_i\left\{\frac{2\left(\frac{b}{a}\right)^2}{\left(\frac{b}{a}\right)^2 - 1}\right\}(P_i - P')\right] \tag{II-10c}$$

For plane strain ($\epsilon_z = 0$):

$$\epsilon_r^{sp} = -\frac{(1-\nu^2)}{E}\left[\left(1 - \frac{\nu}{1-\nu}\right)P_i + \frac{\nu}{1-\nu}K_i\left\{\frac{2\left(\frac{b}{a}\right)^2}{\left(\frac{b}{a}\right)^2 - 1}\right\}(P_i - P')\right] \tag{II-11a}$$

$$\epsilon_\theta^{sp} = \frac{1-\nu^2}{E}\left[-\left(1 - \frac{\nu}{1-\nu}\right)P_i + K_i\left\{\frac{2\left(\frac{b}{a}\right)^2}{\left(\frac{b}{a}\right)^2 - 1}\right\}(P_i - P')\right] \tag{II-11b}$$

An interesting limit case results for incompressible materials ($\nu = \frac{1}{2}$). The first term appearing in the brackets in (II-11a) and (II-11b) will then vanish leaving for plane strain

$$\epsilon_r^{SP} = K_i \epsilon_r(a) \qquad \text{(II-12a)}$$

$$\epsilon_\theta^{SP} = K_i \epsilon_\theta(a) \qquad \text{(II-12b)}$$

Viscoelastic star point strains are obtained from the applicable set of preceding equations in the usual manner by first replacing E and ν by viscoelastic operators and then integrating with respect to time.

A-2. Strain Transformation Equations

Upon internal pressurization, a star-perforated cylindrical propellant grain, case-bonded to a thin elastic metal shell (case), undergoes a deformation which is a function of the actual geometry of the grain and the elastic parameters of the material (assumed purely elastic). The measurement of the strain at the inner surface of the propellant, or more specifically, at the base of one of the star points, is difficult and time consuming.

It is much easier to measure directly the hoop strain at the outer periphery of the metal shell. From this experimental input datum, the maximum hoop strain at the base of a star point can be calculated in the following approximate fashion.

First, the bicomposite cylindrical system is assumed to be long enough that the assumption of plane strain obtains. Secondly, the hoop strain at the outer periphery of the case is transformed to the associated hoop strain at the inner periphery of a circularly perforated cylindrical propellant grain of the same web thickness as that of the star perforated grain. Thirdly, the transformed hoop strain is then modified by the suitable stress concentration factor[5] to obtain the strain at the base of a star point.

The subject of this discussion is the definition of the strain transformation factor (K_ϵ) (from outer case periphery to inner propellant circular periphery). This factor has been reported in sundry literature references[7, 8] to be given by:

$$K_\epsilon = \frac{2\left(\frac{b}{a}\right)^2}{(1+\nu)+(1-\nu)\left(\frac{b}{a}\right)^2} = \frac{2}{(1-\nu)+(1+\nu)\left(\frac{a}{b}\right)^2} \qquad \text{(II-13)}$$

where $1-\frac{a}{b}$ = web fraction of circularly perforated propellant cylinder. In the first progress report (reference 1, page P-8), it was shown that the hoop strain in a circularly perforated hollow cylinder, case bonded, and subjected to external pressure but <u>not</u> internal pressure is given by:

$$\epsilon_\theta \sim \left[(1-\nu)+(1+\nu)\frac{a^2}{r^2}\right]$$

where the proportionality constant is independent of "r". (II-14)

Thus the strain transformation factor defined as $\epsilon_\theta(r=a)/\epsilon_\theta(r=b)$ is identical to equation (II-13), and should <u>not</u> be used for the case of internal pressurization. Actually, its use was first proposed by Durelli in connection with photoelastic experiments carried out at Armour Research Foundation on externally pressurized cylinders.

For an internally pressurized grain, reference 3, page P-12, shows that

$$K_\epsilon = 1+\frac{\left(\frac{b}{a}\right)^2-1}{2(1-\nu)}\left[1+\frac{(1-2\nu)(1+\nu)}{2(1-\nu_c^2)}\frac{E_c}{E}\left(\frac{c^2}{b^2}-1\right)\right] \qquad \text{(II-15)}$$

For the condition $b \gg c - b = t$, equation (II-15) simplifies to

$$K_\epsilon = 1+\frac{\left(\frac{b}{a}\right)^2-1}{2(1-\nu)}\left[1+\frac{(1-2\nu)(1+\nu)}{(1-\nu_c^2)}\frac{E_c}{E}\frac{t}{b}\right] \qquad \text{(II-16)}$$

Assuming both propellant and case are elastic, the following values are inserted into (II-16)

$$\begin{aligned} \nu &= 2/5^{*} \\ \nu_c &= 1/4 \\ E_c &= 3 \times 10^7 \text{ psi} \\ E &= 300 \text{ psi, long-time modulus} \\ b &= 25'', \text{ characteristic of a moderately large motor} \\ t &= .050'', \text{ characteristic of good lightweight design} \end{aligned}$$

which yields

$$K_\epsilon \doteq 1 + \frac{5}{6}\left[\left(\frac{b}{a}\right)^2 - 1\right]\left[1 + 60\right] \simeq 1 + 50\left[\left(\frac{b}{a}\right)^2 - 1\right] \qquad \text{(II-17)}$$

In order to allow for insertion of various values of Young's modulus for propellant, one can write

$$K_\epsilon \doteq 1 + \frac{15000}{E}\left[\left(\frac{b}{a}\right)^2 - 1\right] \qquad \text{(II-18)}$$

Figure (II-2) shows how equations (II-13) and (II-17) compare for $\nu = 2/5$ Note that in both cases, when a = b, $K_\epsilon = 1$. However, as a $\longrightarrow$ 0 (solid cylinder), the Durelli transformation factor approaches $(2/1-\nu)$, whereas the appropriate factor approaches infinity. Since the Durelli factor is often mistakenly cited in the literature as applicable to the case of an internally pressurized grain, it follows that many hoop strains have been underestimated. Care should be exercised to use the correct factor given by equation (II-16).

---

*This value of $\nu = .4$ is based on analysis of true strain data obtained in the ambient temperature range at Aerojet-General Corporation on a large number of composite polyurethene-bound aluminized solid propellants.

B. Effect of Temperature upon Liner-Propellant Bond Stress

The liner is an important component of rocket motors for two reasons. It serves to bond the propellant to the metal case, and for this reason, must be capable of sustaining any normal or shear stresses that develop at the propellant-liner and/or liner-case interfaces. Secondly, its presence demands that the grain be of the internal-burning type, the port profile of which must be irregularly perforated in order to establish constancy of burning area during the duration of flight. This variation in radius of curvature of the port periphery makes for stress concentrations and also shear stresses in the web of the grain and imposes further demands upon the character of the propellant-liner bond. In this section, only the effect of thermal contraction upon the liner-propellant bond stress for the case of circularly perforated grain will be considered. The next quarterly report will take up the question of the stresses that arise as a result of thermal contraction in a star perforated grain.

Following the method outlined by Prof. K. S. Fister (reference 3, page P-19), it is easily shown that the normal radial stress at the propellant-liner interface (r = b) is given by:

$$\frac{\sigma_r(b)}{-\Delta T} = \frac{\frac{2}{3}\mu''\epsilon''(1+\epsilon')(\alpha-\alpha'') - \mu'\epsilon'(\alpha'-\alpha)}{\frac{1+\epsilon'}{2} + \frac{1-2\nu+\lambda}{1-\lambda}\epsilon''(1+\epsilon')\frac{\mu''}{3\mu} + \frac{1-2\nu+\lambda}{1-\lambda}\frac{\epsilon'}{2}\frac{\mu'}{\mu}} \qquad \text{(II-19)}$$

where

non prime refers to propellant
single prime refers to liner
double prime refers to case
μ = shear modulus
α = linear coefficient of thermal expansion
ν = Poisson's ratio

$$\lambda = \frac{a^2}{b^2}$$

$$\epsilon' = \frac{d^2}{b^2} - 1$$

$$\epsilon'' = \frac{c^2}{d^2} - 1$$

a = inner or port radius of propellant grain

b = outer radius of grain or inner radius of liner

c = outer radius of case

d = outer radius of liner or inner radius of case

Reasonable assumptions (based on experimental values) for the thermal and mechanical parameters are given as follows:

$\alpha = 55 \times 10^{-6}$ in/in/^{o}F

$\alpha' = 140 \times 10^{-6}$

$\alpha'' = 7 \times 10^{-6}$

$\lambda = 1/4$, an arbitrarily chosen example

$\nu = 2/5$, based on recent intensive studies at Aerojet-General Corp.

$\mu''/\mu' = 10^5$

$\epsilon'' = .004$, typical of a moderately large motor

Substitution of these values into (II-19) reveals that it may be well approximated by

$$\frac{\sigma_r(b)}{-\Delta T} = \frac{2\mu(\alpha-\alpha'')(1-\lambda)}{1-2\nu+\lambda} = \frac{E(\alpha-\alpha'')(1-\lambda)}{(1-2\nu+\lambda)(1+\nu)} \qquad \text{(II-20a)}$$

Thus the minimum required liner-propellant bond strength is virtually insensitive to the thickness of the liner as well pointed out by Pister[3]. For the particular values tabulated above, (II-20a) becomes

$$\sigma_r(b) = (-E\Delta T)\, 57 \times 10^{-6} \text{ psi} \qquad \text{(II-20b)}$$

Figure (II-3) shows how Young's modulus depends on temperature for a typical composite propellant based on polyurethane binder filled with 60 ^{o}/o ammonium perchlorate, and 15 ^{o}/o aluminum. Figure (II-4) shows how the normal radial stress, which must not exceed the minimum

liner-propellant adhesion strength, varies with temperature in a motor about 50" in diameter. The reference temperature at which all stresses are zero is taken to be 110°F. It is important to note that the temperature range -10°F to -40°F which corresponds to the range of available liner-propellant bond strengths, is also the range below which many case-bonded rocket motors develop failure problems.

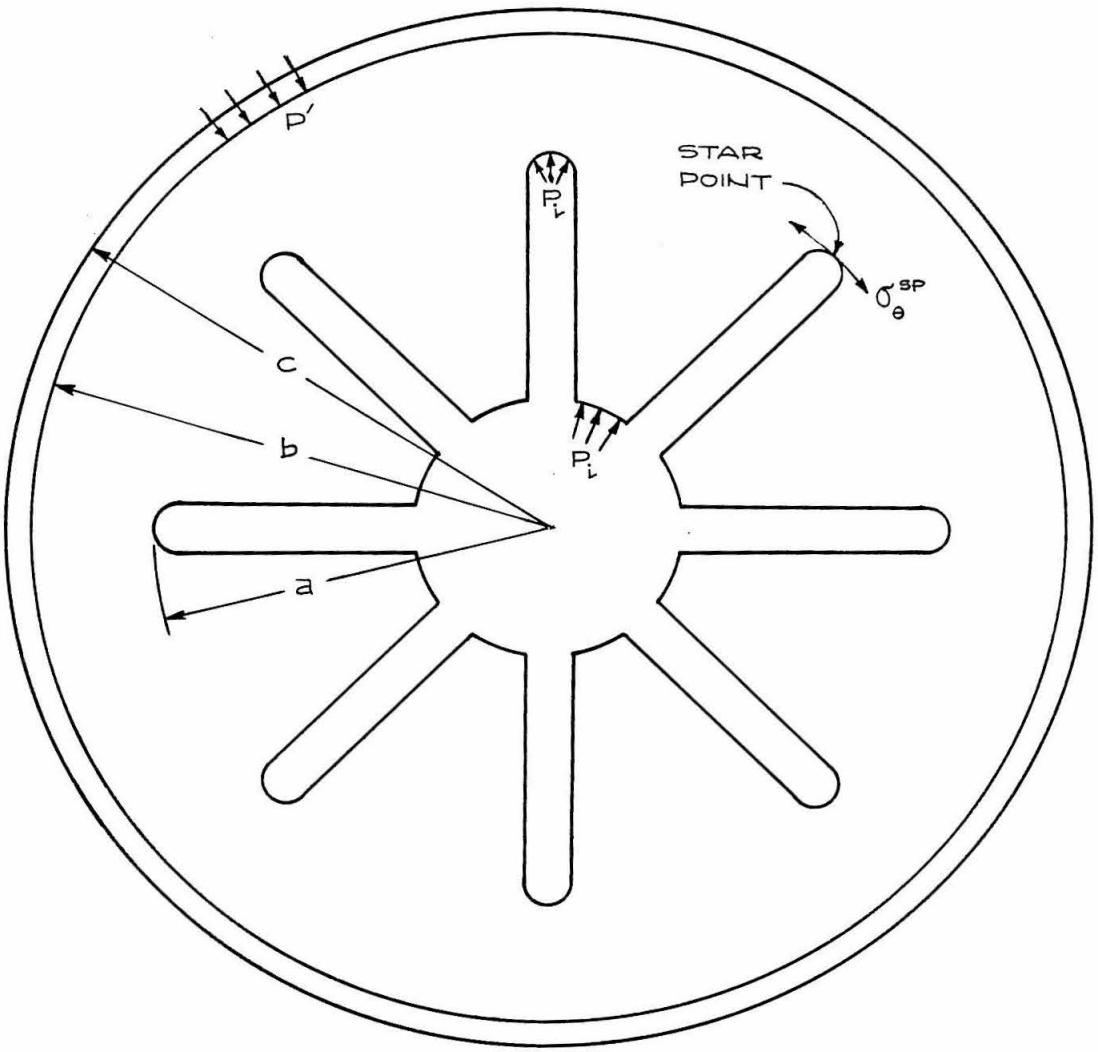

FIG. II-1. CASE-BONDED GRAIN WITH INTERNAL STAR-SHAPED PERFORATIONS

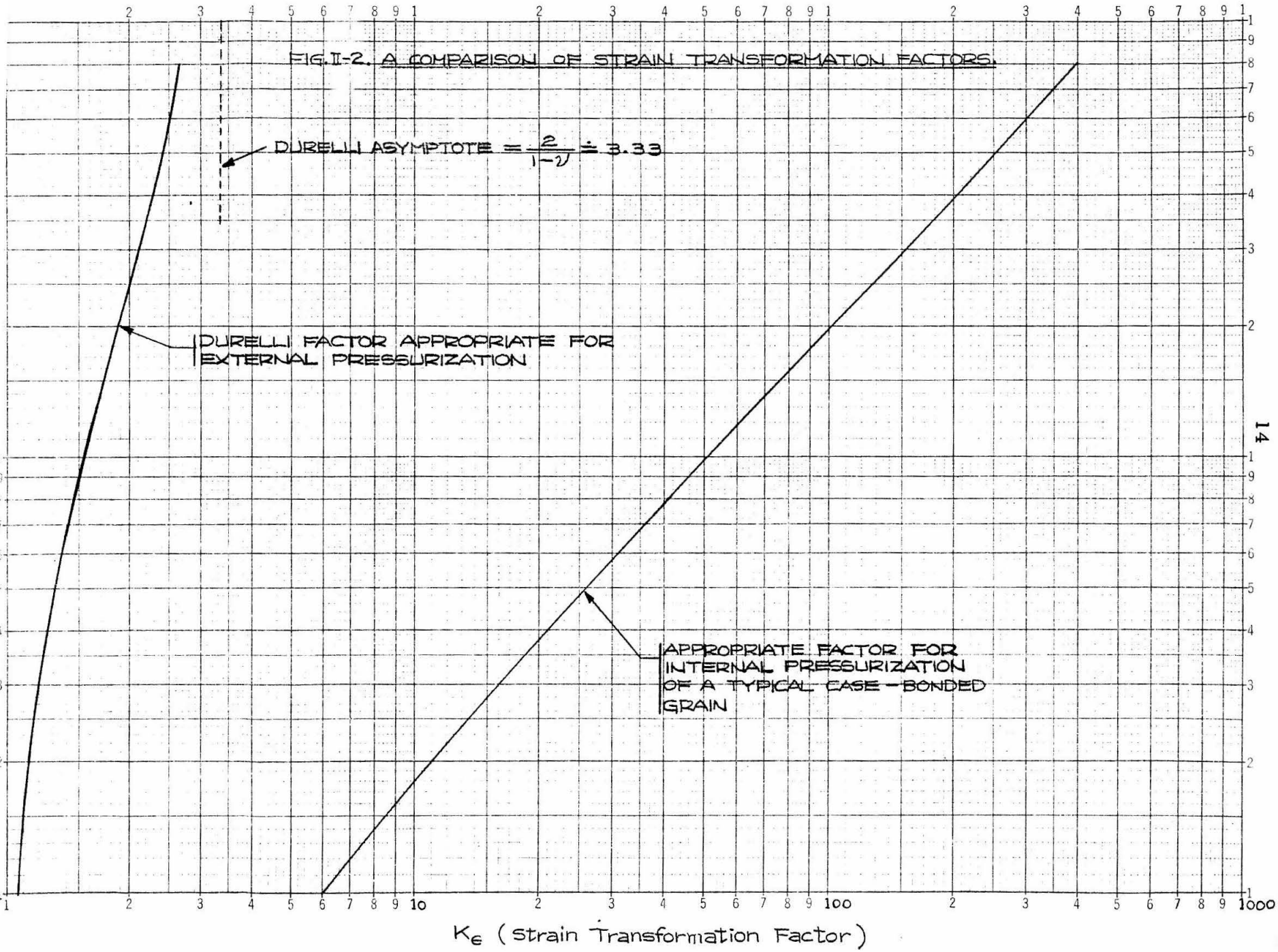

FIG. II-2. A COMPARISON OF STRAIN TRANSFORMATION FACTORS.

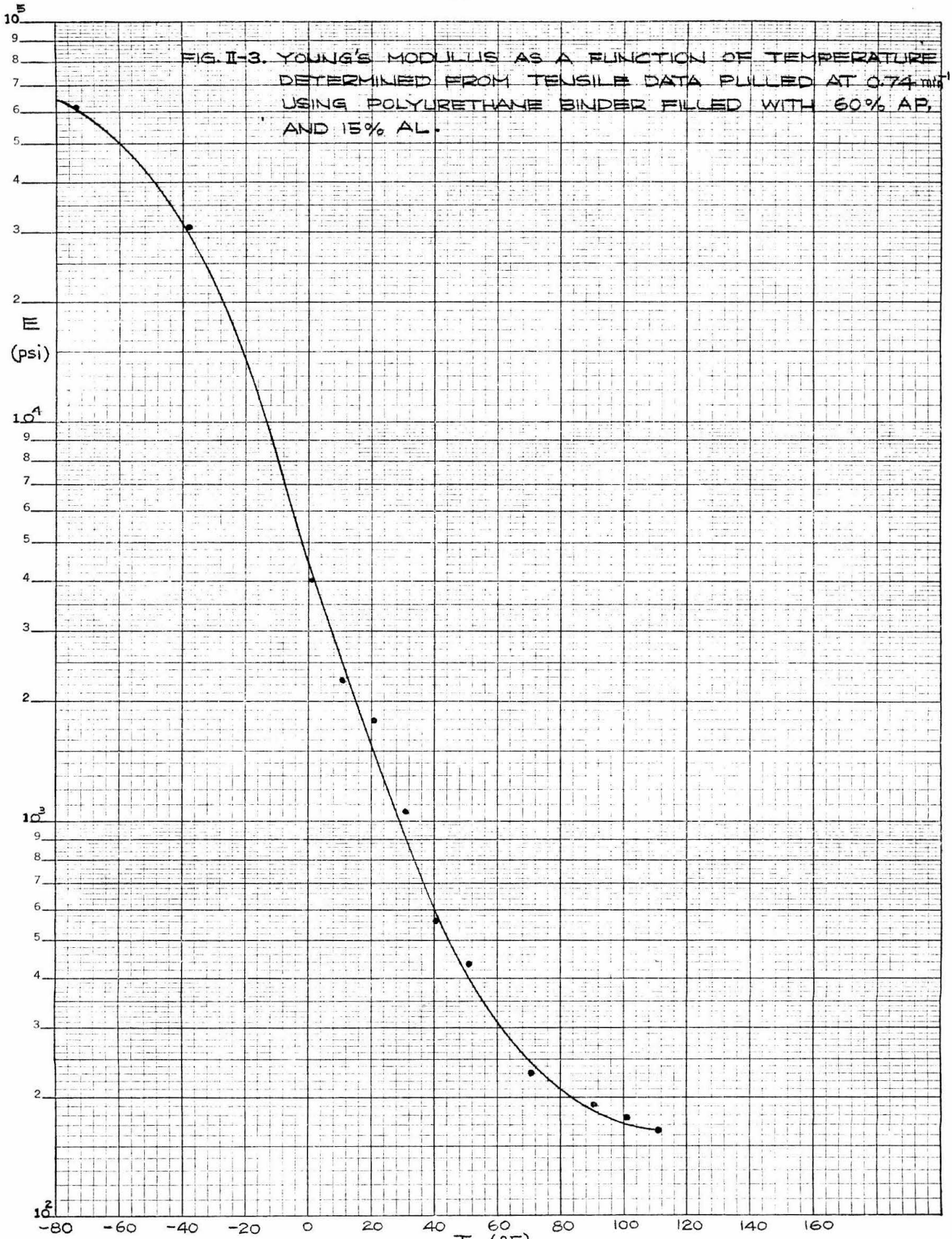

FIG. II-3. YOUNG'S MODULUS AS A FUNCTION OF TEMPERATURE DETERMINED FROM TENSILE DATA PULLED AT 0.74 min^{-1} USING POLYURETHANE BINDER FILLED WITH 60% AP, AND 15% AL.

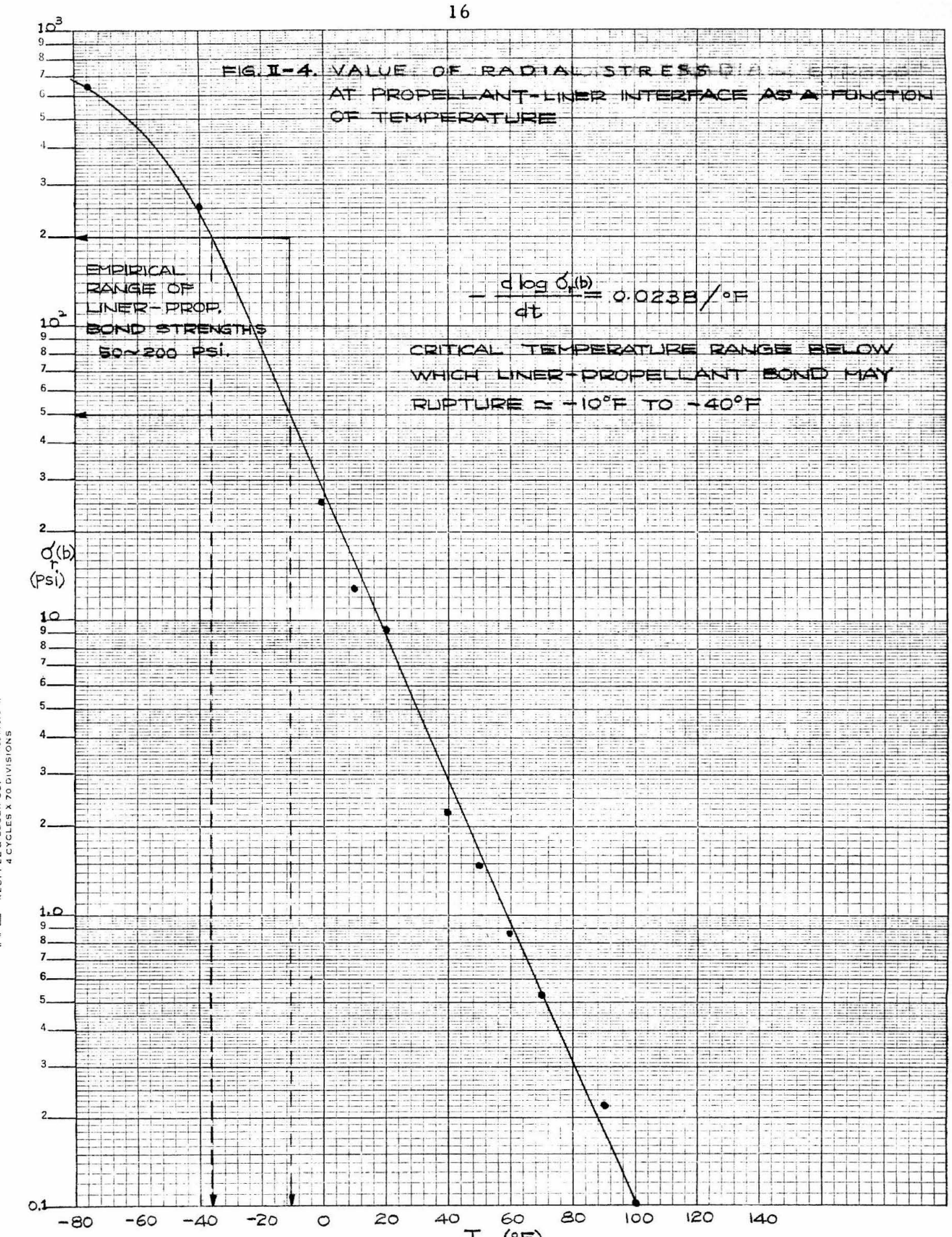
FIG. II-4. VALUE OF RADIAL STRESS AT PROPELLANT-LINER INTERFACE AS A FUNCTION OF TEMPERATURE
EMPIRICAL RANGE OF LINER-PROP. BOND STRENGTHS 50~200 PSI.
$-\frac{d \log \sigma_r^{(b)}}{dt} = 0.023 B/°F$
CRITICAL TEMPERATURE RANGE BELOW WHICH LINER+PROPELLANT BOND MAY RUPTURE ≃ -10°F TO -40°F
$\sigma_r^{(b)}$ (psi)
T (°F)
-80 -60 -40 -20 0 20 40 60 80 100 120 140
4 CYCLES X 70 DIVISIONS

IV. ENGINEERING ANALYSIS

A. Example of Viscoelastic Strains in Star Grain upon Ignition

The approach for determining pressure strains in a star grain upon ignition begins with the elastic solution for a hollow cylindrical grain bonded in a thin case (incompressible and plane strain in this example):

$$\sigma_{(r\theta)} = \frac{\mp\left(\frac{b}{r}\right)^2 + 1 - \frac{(3/2)}{1-\nu_c^2}\frac{hE_c}{bE}}{\left(\frac{b}{a}\right)^2 - 1 + \frac{(3/2)}{1-\nu_c^2}\frac{hE_c}{bE}} P_i \qquad \text{(IV-1)}$$

where the upper sign is for σ_r and lower sign for σ_θ. The viscoelastic model, which is used to convert the above elastic solution into a viscoelastic solution, normally would be obtained from experimental data by procedures to be presented at a later date. A simple Voigt model having an appreciable time lag is assumed; time lag was chosen for illustrative purposes only and may not correspond to any given propellant material. The operator equation is given in Table I of reference 1.

$$\overline{\tau}_{ij} = (\eta p + \mu)\,\overline{\gamma}_{ij} \qquad (i \neq j) \qquad \text{(IV-2)}$$

Replacing the modulus E in equation (IV-1) by its equivalent $3(\eta p + \mu)$ in equation (IV-2), we have the result:

$$\overline{\sigma}_{(r\theta)} = -\frac{\left[\pm\left(\frac{b}{r}\right)^2 - 1\right](\eta p + \mu) + \frac{hE_c}{2(1-\nu_c^2)b}}{\left[\left(\frac{b}{a}\right)^2 - 1\right](\eta p + \mu) + \frac{hE_c}{2(1-\nu_c^2)b}}\,\overline{P}_i(p) \qquad \text{(IV-3)}$$

which, incidentally, is the result on page 6 of reference 3.

Another form of pressure input has been assumed which generalizes the ignition transient and results in more uniform changes in strain-rate (more appropriate for rate dependence in failure):

$$P_i = P_c\left[1 - e^{-mt}\cos nt\right] \tag{IV-4}$$

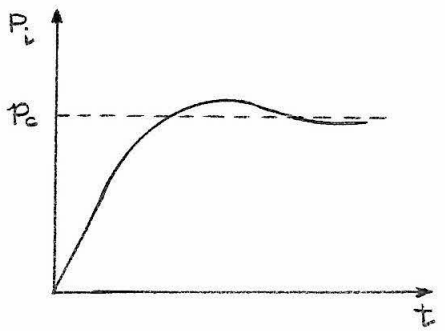

with a transform

$$\overline{P_i}(P) = P_c\left[\frac{1}{P} - \frac{P+m}{(P+m)^2+n^2}\right] \tag{IV-5}$$

Substituting (IV-5) into (IV-3) and simplifying:

$$\overline{\sigma}_{(r_\theta)} = k P_c\left[\frac{P+a_o}{P+\alpha}\right]\left[\frac{1}{P} - \frac{P+m}{(P+m)^2+n^2}\right] \tag{IV-6}$$

where

$$k \equiv -\frac{\pm\left(\frac{b}{r}\right)^2 - 1}{\left(\frac{b}{a}\right)^2 - 1}$$

$$a_o \equiv \frac{\mu}{\eta} + \frac{hE_c}{2\eta(1-\nu_c^2)b\left[\pm\left(\frac{b}{r}\right)^2 - 1\right]} \tag{IV-7}$$

$$\alpha \equiv \frac{\mu}{\eta} + \frac{hE_c}{2\eta(1-\nu_c^2)b\left[\left(\frac{b}{a}\right)^2 - 1\right]}$$

The inversion of equation (IV-6) is rather lengthy with the final result:

$$\sigma_{(r_\theta)}(t) = kP_c\left\{\frac{1}{\alpha}\left[a_o - (a_o-\alpha)e^{-\alpha t}\right] - \frac{\alpha^2 - (m+a_o)\alpha + ma_o}{(\alpha-m)^2+n^2}e^{-\alpha t}\right. \tag{IV-8}$$
$$\left. - \sqrt{\frac{(a_o-m)^2+n^2}{(\alpha-m)^2+n^2}}\, e^{-mt}\sin(nt+\phi_{(r_\theta)})\right\}$$

where

$$\phi_{(r_\theta)} = \tan^{-1}\left[\frac{(\alpha-m)(a_o-m)+n^2}{(a_o-\alpha)n}\right]$$

and (assuming incompressibility):

$$\sigma_z(t) = \frac{1}{2}\left[\sigma_r(t) + \sigma_\theta(t)\right] \qquad \text{(IV-9)}$$

The hoop strain from plane strain elastic theory is:

$$\epsilon_\theta = \frac{(1+\nu)}{E}\left[(1-\nu)\sigma_\theta - \nu\sigma_r\right] = \frac{3}{4E}\left[\sigma_\theta - \sigma_r\right] \quad \text{for } \nu = \frac{1}{2} \qquad \text{(IV-10)}$$

and its operational form is:

$$\overline{\epsilon}_\theta(P) = \frac{3}{4\overline{E}(P)}\left[\overline{\sigma}_\theta(P) - \overline{\sigma}_r(P)\right] \qquad \text{(IV-11)}$$

To substitute the operational stresses from equation (IV-6) and the equivalent modulus from equation (IV-2) into equation (IV-11) and Laplace invert the result would be considerable effort. Thus, as an expediency to show general results, we have used equation (IV-10) with the time-dependent stresses from equation (IV-8) and an average modulus for E. The "viscoelastic" strains are simply multiplied by the appropriate stress concentration factor for the incompressible case as demonstrated in Section II of this report. A four pointed star with point radius $\rho = a/6$ and $(b/a)^2 = 10$ was chosen as an example with a resulting stress concentration factor, K_i, equal to about two. The star-point, viscoelastic strains are shown in Figure IV-1 for a range of moduli and corresponding pressure rate conditions.

FIG. IV-1: VISCOELASTIC STRAINS IN A STAR GRAIN UPON IGNITION

$$P_i = P_c\left[1 - e^{-mt}\cos nt\right]$$

I $m=1$ $n=1.2$, $E=10^3$ psi

II $m=10$ $n=12$, $E=10^4$ psi

III $m=100$ $n=120$, $E=10^5$ psi

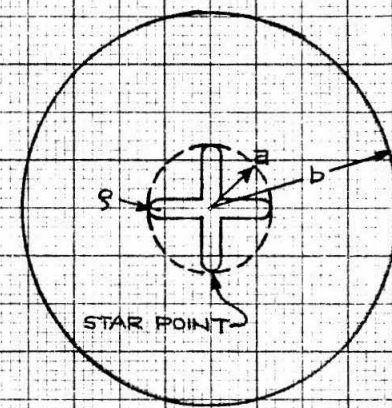

$\left(\frac{b}{a}\right)^e = 10$

$\rho = \frac{a}{b}$

$\frac{W}{b} = 68\%$

$\frac{b-a}{\rho} = 13$

V. FAILURE CRITERIA

Introduction

The previous progress report[3] presented a survey of the problems involved in predicting failure in solid propellant grains. For the most part, initial interests have centered on the mechanical rupture of propellants under various loading conditions. It is important to realize that failures in solid propellant motors are not necessarily a result of rupturing or cracking of the grain. In fact, some partially cracked grain motors have fired within the acceptable performance limits, while other grains have fired with no apparent rupture and have failed with evidence pointing toward failure due to the physical properties of the grain. To be of practical use, a failure criterion must eventually take into account these factors; however, we are initially restricting our interests to the propellant rupture problem.

In the previous report, a need for a variety of tests was discussed. These tests will be amplified at a later date in Section I and in correspondence regarding them, however it is the purpose of this section to develop failure criteria based upon theory and testing. As a start, a generalization of the Smith[8] failure criterion for polymeric substances was suggested[3]. This included extensions to specific propellants, to varying strain-rates, and to biaxial and triaxial loadings. A series of tests on a propellant (rather than rubber or polyisobutylene) similar to Smith's is appropriate. This should include a variety of strain-rates, different temperatures, and an investigation to yield effective gage lengths and localized strains.

The extension to variable strain-rate is being investigated through the use of the cumulative damage concept discussed in the previous report[3]. A section follows which presents results from some preliminary tests on an Instron in which different strain-rates were used on the same sample. This effort should be expanded in terms of quantity of tests for statistical reasons and tried on significantly different types of propellant. In addition, this should be expanded to various temperatures and higher rates. Finally, it is desirable to perform more typical continuously varying rates,

rather than abrupt changes.

The extension to biaxial and triaxial loading was mentioned in the previous report[3]. Some such tests are the hollow tube under torsion,[9] photographing grids on tensile specimens to obtain shear data, tensile specimens with hydrostatic pressure imposed on the sides, large sandwich plates with propellant between being pulled normal to their plane, and the thick walled cylinder bonded in a thin case under internal pressure or under temperature cycling. The hollow tube and photographic tensile tests are biaxial, while the others are primarily triaxial. The first two tests can yield shear modulus in contrast to the uniaxial tension modulus. The tensile specimen with hydrostatic pressure superimposed approximates the hoop "specimen" inside a rocket grain under internal pressure, whereas the sandwich (or pancake) test approximates the behavior of a specimen submerged in a grain under thermal cooling. The thick walled cylinder approximates an actual rocket grain and can be extended to this through the use of stress concentration factors discussed in Section II.

Cumulative Damage

Smith[8] based a failure criterion on strain and strain-rate, including temperature as a sliding scale. However, his tests on GR-S rubber and polyisobutylene were performed at the same constant strain-rate all the way to break. It is the purpose of this section to elaborate on a possible extension of tensile testing to variable strain-rate in predicting fracture.

It was suggested in the previous progress report[3] that propellant samples in failure tests may accumulate damage, and that the basis for accumulation might be any number of measurable quantities such as strain, time or energy.* The cumulative concept as suggested for Instron strain-rate tests is as follows. Suppose two different samples are strained, one at a higher strain-rate than the other. Both are strained at their respective rates all the way to failure.

---

*The strain basis is identical to the time basis (used in the previous progress report) in the constant strain-rate tests described here.

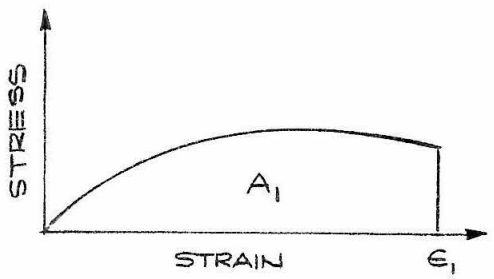

LOWER RATE $= R_1$

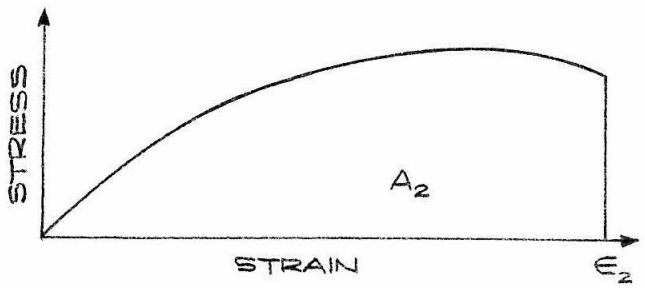

HIGHER RATE $= R_2$

Now suppose, instead, that the first sample had been strained at its rate, R_1, only part way and then strained the remainder of the way at the higher rate, R_2.

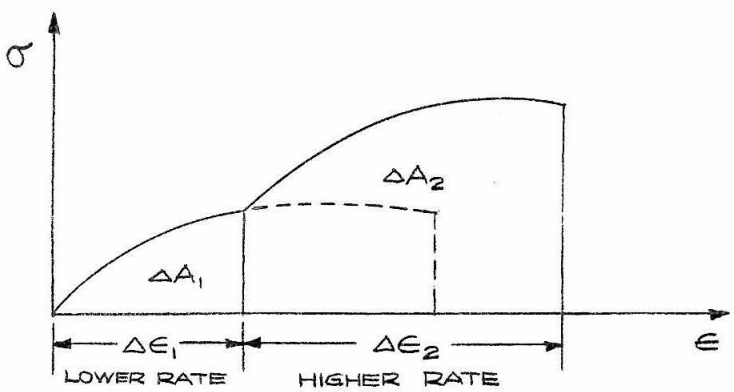

Accumulation based on strains then is:

$$\frac{\Delta\epsilon_1}{\epsilon_1} + \frac{\Delta\epsilon_2}{\epsilon_2} = 1$$

whereas based on energy $= \int \sigma d\epsilon$ = areas under curves:

$$\frac{\Delta A_1}{A_1} + \frac{\Delta A_2}{A_2} = \frac{\int^{\Delta\epsilon_1} \sigma d\epsilon}{\int^{\epsilon_1} \sigma d\epsilon} + \frac{\int^{\Delta\epsilon_2} \sigma d\epsilon}{\int^{\epsilon_2} \sigma d\epsilon} = 1$$

Some preliminary testing is being performed on polyurethane propellant tensile specimens at the Jet Propulsion Laboratory to check the feasibility of the cumulative damage concept from Instron testing. Several samples have been run at various strain-rates and some have been run with midpath changes in strain-rate. Figure V-1 is a typical run in which three different strain-rates were used.

In spite of the few tests made with noticeable scatter in the results and certain shortcomings in the technique of changing rate, the results show that accumulation based on either strain or energy appears feasible. It is felt that there will be more means for determining the best basis of accumulation at strain-rates higher than feasible on Instron equipment. Runs at lower temperatures and moderate rates on an Instron may also produce a similar result. Certainly many more runs need to be made in order to account for the statistical variation in propellant specimens.

Table V-1 presents the results from some of the preliminary tests showing the values obtained upon accumulation based on strain and energy. A value of unity represents an accurate cumulative result, whereas spreads of values are due, in part, to sample variation. A slight bias above unity seems to exist and has been found to be even larger in the latest runs which suggests non-linear accumulation may be more accurate. Roughly speaking, the initial sample variations are at most about $\pm$ 10 ^{o}/o whereas the cumulative spreads are about $\pm$ 20 ^{o}/o. The actual standard deviations are shown and about double in the cumulative process. This increase in spread is expected and corresponds with that found in metal fatigue tests.

In order to make Table V-1 more understandable, consider the first accumulation run, no. 1878. Preliminary tests made separately at 74 ^{o}/o strain/min and at 7.4 ^{o}/o strain/min all the way to failure resulted in mean values for strain to break of 64 ^{o}/o and 41 ^{o}/o, respectively. In run no. 1878 a specimen was strained at the first rate until it had reached 32 ^{o}/o elongation or half its potential strain. Then it was continued at the second (lower) rate until break which was an additional 24.5 ^{o}/o elongation (based on original length). Performing the accumulation based

on strain,

$$\frac{32\ ^{o}/o}{64\ ^{o}/o} + \frac{24.5\ ^{o}/o}{41\ ^{o}/o} = 1.10$$

which appears under the total accumulation column. The energy accumulation was performed in a similar way with 53^{o}/o of the potential energy occurring during the first strain-rate and 49 ^{o}/o during the second (based on total energies at the respective constant rates from previous tests taken all the way to break). These energy percentages are tabulated immediately below the strain-rates in the table.

It appears that the basis for cumulative damage can be investigated theoretically through the aid of viscoelastic models containing springs and dashpots. The energy basis, and probably the distortion energy, is particularly advantageous in that elastic energy and dynamic (dashpot) energy can be distinguished and permits a generalization to biaxial and triaxial loadings. It is expected that the model approach will give deeper insight into the theory of cumulative damage and include relaxation effects which are quite evident during rate change (see regions A and B in Figure V-1).

TABLE V-1 CUMULATIVE DAMAGE

Run No.	Strain Rates (in/in/min) % Accumulated at each S.R. (Energy Basis) 1st	2nd	3rd	4th	Total Accumulation Strain Basis	Energy Basis	Standard Deviations Energy Basis	Initial Data
1878	.74	.074						
	53	49			1.10	1.02		
1879	.074	.74						
	46	51			.97	.97		
1880	.74	.074						
	51	36			.88	.87		
1881	.074	.74						
	43	85			1.38	1.28	0.14	0.07
1882	.74	.074						
	20	66			.84	.86		
1883	.074	.74						
	14	83			.99	.97		
1884	.74	.074						
	19	77			.97	.96		
1955	.037	.37						
	41	64			1.11	1.05		
1956	.037	.37						
	42	68			1.14	1.10		
1957	.37	3.7						
	53	30			.79	.83		
1958	.37	3.7						
	19	105			1.41	1.24	0.18	0.08
1959	.037	3.7						
	41	72			1.21	1.13		
1960	.037	3.7						
	13	64			.78	.77		

TABLE V-1 CUMULATIVE DAMAGE (continued)

Run No.	Strain Rate (in/in/min) % Accumulated at each S.R. (Energy Basis) 1st	2nd	3rd	4th	Total Accumulation Strain Basis	Energy Basis	Standard Deviations Energy Basis	Initial Data
1961	.037	.37	3.7					
	14	30	70		1.20	1.14		
1962	.037	.37	3.7					
	13	31	54		1.02	.98		
1963	.037	.37	3.7				0.11	0.08
	28	50	34		1.09	1.12		
1964	.037	.37	3.7					
	44	32	27		.97	1.03		
2093	.0074	.074	.74					
	19	39	54			1.12		
2094	.0074	.074	.74					
	11	30	67			1.08		
2095	.0074	.074	.74					
	23	48	51			1.22		
2096	.0074	.074	.74					
	17	48	63			1.18		
2097	.0074	.074	.74	7.4			0.17	0.07
	5	8	19	87		1.19		
2098	.0074	.074	.74	7.4				
	3	7	18	101		1.29		
2099	.0074	.074	.74	7.4				
	1	6	21	81		1.09		
2100	.0074	.074	.74	7.4				
	8	9	19	77		1.13		

FIG. V-1. LOAD VS. TIME RUN NO. 1961

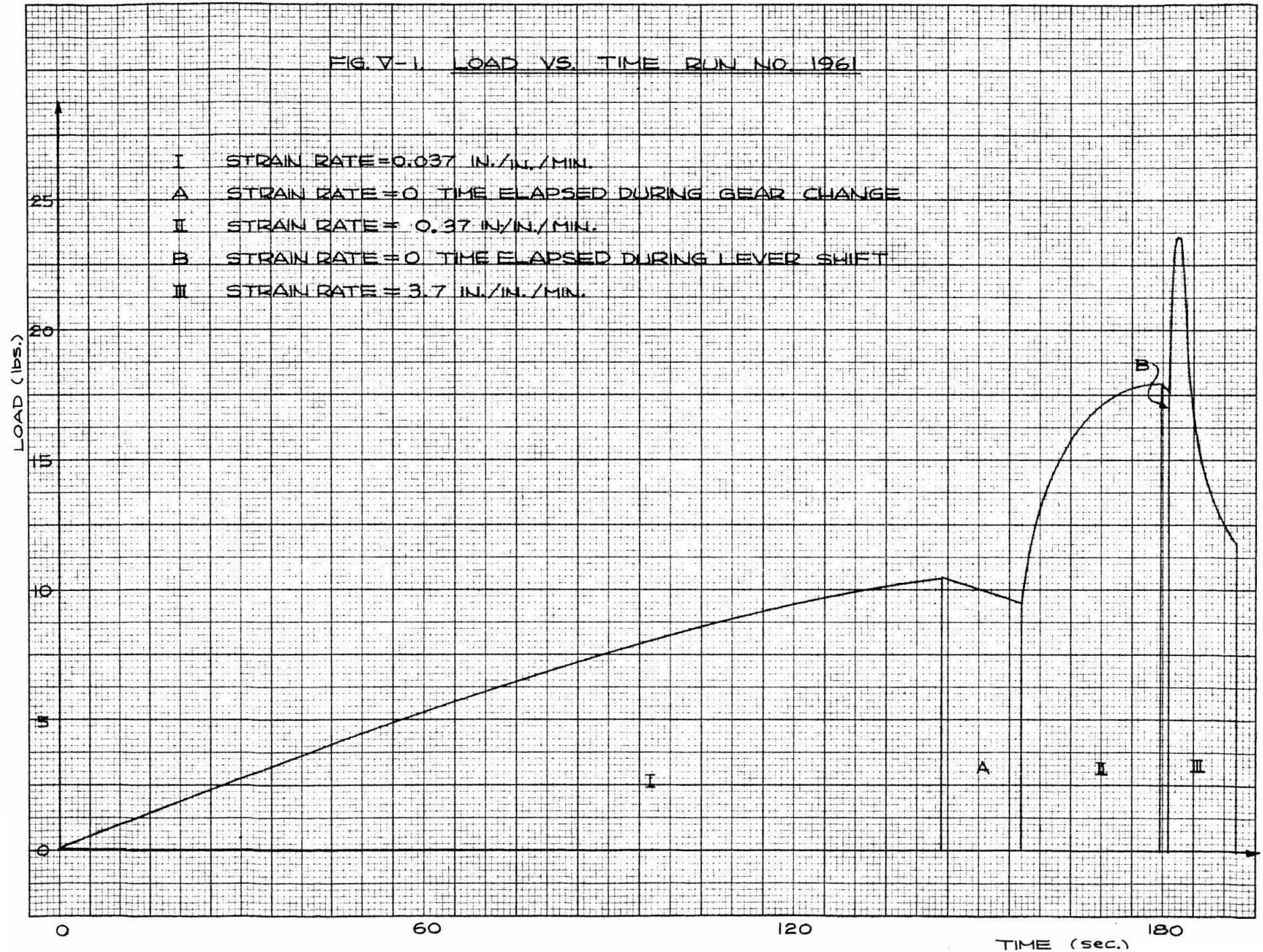

REFERENCES

1. R. A. Schapery, L. D. Stimpson, M. L. Williams, "Fundamental Studies Relating to Systems Analysis of Solid Propellants", California Institute of Technology, GALCIT 101, Progress Report No. 1, January 15, 1959.

2. R. A. Schapery, L. D. Stimpson, M. L. Williams, "Fundamental Studies Relating to Systems Analysis of Solid Propellants", California Institute of Technology, GALCIT 101, Progress Report No. 2, April 15, 1959.

3. R. A. Schapery, L. D. Stimpson, M. L. Williams, "Fundamental Studies Relating to Systems Analysis of Solid Propellants", California Institute of Technology, GALCIT 101, Progress Report No. 3, July 15, 1959.

4. E. H. Lee, "Viscoelastic Stress Analysis", Brown University, NR-064-406, July 1958.

5. D. D. Ordahl, M. L. Williams, "Preliminary Photoelastic Design Data for Stresses in Rocket Grains", Jet Propulsion, June 1957.

6. S. Timoshenko and J. N. Goodier, "Theory of Elasticity", p. 59. McGraw-Hill Book Company, Inc., New York, 1951.

7. R. M. Pierce, Hughes Aircraft Co., Proceedings of the 13th Meeting of JANAF panel.

8. T. L. Smith, "Elastomeric-Binder and Mechanical Property Requirements for Solid Propellants", California Institute of Technology, Jet Propulsion Laboratory Memo. No. 20-178, January 7, 1959.

9. W. Dowler, G. Lewis, L. D. Stimpson, "Torsion Testing of Solid Propellants", California Institute of Technology, Jet Propulsion Laboratory Publ. No. 30-4, April 24, 1959.